ISSN 0915-633X

NATIONAL INSTITUTE FOR FUSION SCIENCE

Fast Ion Loss and Radial Electric Field in Wendelstein VII-A Stellarator

K. Itoh, H. Sanuki and S.-I. Itoh

(Received – Sep. 20, 1991)

NIFS-117 Oct. 1991

RESEARCH REPORT
NIFS Series

NAGOYA, JAPAN

Fast Ion Loss and Radial Electric Field in Wendelstein VII-A Stellarator

K. Itoh, H. Sanuki and S.-I. Itoh

National Institute for Fusion Science, Nagoya 464-01, Japan

Abstract

Theoretical model is developed to determine the radial electric field and the fast ion loss simultaneously in stellarators, and is applied to the Wendelstein VII-A stellarator. The predicted value of the radial electric field is more closer to experiments than the purely neoclassical calculation. The loss rate, which is determined simultaneously, is in the range of experimental observations. The partition of the injection energy by the bulk heating, direct orbit loss and shine through is estimated by using the self consistent electric field profile. The orbit loss become noticeable as the injection energy increases. The influence of the neutral particles is also studied. Neutral particles enhances the negative radial electric field, and reduces the direct orbit loss by the expense of the charge exchange loss. The impact of the increased radial electric field on the neoclassical ion thermal energy loss is compared to the direct loss of fast ions. The reduction of the neoclassical loss is much smaller than the orbit loss.

Keywords: Stellarator, Fast Ion Loss, Loss cone, Radial Electric Field, Charge Exchange Loss, Neoclassical Transport, Wendelstein VII-A,

§1 Introduction

The important roles of the radial electric field in stellarators (helical systems) have been widely known. Motivation for the analysis on the radial electric field was first given from the improved absolute trapping of particles[1-3] (i.e., reduction of the loss cone), and then as a result of this, the reduction of neoclassical thermal transport[4-6] was another strong drive for the investigations. Experiments in Wendelstein VII-A (WVII-A) has shown that, even though the anomalous transport prevails, the reduced loss was observed in NBI heated discharges in which the radial electric field was piled up as well[7,8]. The reduction of the neoclassical ion heat flux has been discussed[7]. The reduced fluctuation has also been observed[9]. The causality between the reduction of the anomalous loss and the radial electric field has not been confirmed yet, but the recent observations and modelling on H-mode in tokamaks[10-12] also encourage the study of the radial electric field associated with the energetic particle loss.

The poloidal gyroradius of fast ions generated by the NBI in WVII-A stellarator is compatible with the minor radius, and the trapping (and hence the plasma heating) is very difficult without the help of radial electric filed. The influence of the observed radial electric field on the orbit was studied, and the potential difference of about 1keV is enough to confine this energetic particles[13,14]. The selfconsistent analysis, which determines the loss of energetic particle and electric field simultaneously, has not been performed, although the importance of the research of this kind was recognized. The analysis on the radial electric field in helical systems has shown that neutral particles and anomalous loss flux are also important[15,16]. In a preceding article, we present a simple analytic theory for the equation to determine the loss boundary of energetic particle[17]. The radial electric field is determined by the procedure in which loss cone current is balanced with the neoclassical current. This analysis gives the radial profile and loss rate of fast ions simultaneously.

In this article, We apply this method to the NBI heated plasma in WVII-A. The fraction of the loss particle, and hence the radial electric field itself, depend on the birth profile of fast ions. Using the experimentally obtained density and temperature profiles, we evaluate the selfconsistent radial electric field, keeping the fast ion loss. The partition between the ratio of the bulk heating, direct orbit loss and the shine through is evaluated. Dependence on the injection energy is also discussed. Higher injection energy increases the radial electric field for fixed plasma parameters. We find the potential difference of the order of 1keV and the loss rate of fast ion orbit loss of about 30%, which is in the range of experimental observations. We also study the influence of the neutral particles, which make the radial electric field more negative[18,19]. The fast ion loss enhances the radial electric field and reduces the neoclassical bulk ion loss. This reduction in the ion heat loss,however, is much smaller than the power taken away by the direct orbit loss.

§2 Model

The WVII-A stellarator[7] has the very high aspect ratio, $R/a=20$, and medium rotational transform, $\iota = 1/3 \sim 1/2$. (a is the minor radius and R is the major radius). The poloidal gyroradius ρ_p of the hydrogen ion with the injection energy of $W_b=28keV$ reaches about 30cm (at $B_T=2.5T$) exceeding the minor radius of a=10cm. Substantial part of the injection power is carried by the particles with the energy of $W_b/2$ or $W_b/3$, but almost all of them enter the loss cone in the absence of radial electric field.

In the limit where the poloidal motion of particles is dominated by the E×B rotation, not by the parallel motion, the location in the poloidal cross section is dictated by the equation[20,21]

$$\Psi(r,\theta) = [rW/eB_0R]\cos\theta - \Phi/B_0 = \text{constant} \qquad (1)$$

where r is the minor radius, e is elementary charge, θ is the poloidal angle, and Φ is the static potential which is the function of r.

We define the loss cone by the condition that the particles starting from r=r, θ=0 (or θ=π) reaches to r=b at some poloidal angle. (b > a). The loss cone boundary r_* is defined by the condition that particles generated at the radius $r>r_*$ enter the loss cone and those bone in the region $r<r_*$ do not. We are interested in the case that the static potential is a monotonous function of the minor radius. [Note that we need not to assume

that Φ is parabolic.] In case of the negative radial electric field, which is realized in the NBI heated plasmas, the loss cone appears in the inner side of the torus ($\theta=\pi$). Substituting (b, 0) and (r_*, π) in the left hand side of Eq.(1), we have the relation by which the loss cone boundary is determined as

$$[\Phi(b) - \Phi(r_*)]e/W = (b+r_*)/R. \qquad (2)$$

From this relation, we see the lower boundary for the potential barrier, which is necessary to prevent the loss cone from touching the magnetic axis, as

$$e[\Phi(b) - \Phi(0)] > (b/R)W. \qquad (3)$$

In the region $r>r_*$, there exists the radial current associated with the loss cone loss. In this article, we choose a simple model of injected beam, such that the birth profile is limited on the equatorial plane and the radius of the beam channel is neglected. The power flux P(x) is the injection power across the surface $x=r\cos\theta$. Under this simplified situation, we have derived a form of the radial current associated with the loss cone in a previous article[16,17] as

$$\Gamma_{lc}(r) = [P(-r)-P(-r_*)]/4\pi^2 RrW_b \qquad (4)$$

where the suffix lc indicates the loss cone, and the minus value of the argument of P implies that the loss cone exists in the high field side of the torus for $E_r<0$. Figure 1 illustrates the drift orbit $\Psi(r,\theta)$=const, the loss cone boundary r_*, and the birth profile of fast ions, $S_i(x)$, schematically. The particle source which is born in the region $[-r, -r_*]$ contributes to the radial current by the loss cone at $r=r$. It is noted that the partition between the shine through, direct orbit loss, charge exchange loss, and bulk heating is given by the following ratios as

$$\eta_{st} = P(-a)/P(a) \tag{5-1}$$

$$\eta_{ol} = [P(-r_*)-P(-a)]/P(a) \tag{5-2}$$

$$\eta_{cx} + \eta_{bh} = 1 - P(-r_*)/P(a) \tag{5-3}$$

where suffix st, ol, cx and bk denote the shine through, orbit loss, charge exchange, and bulk heating, respectively. These ratios satisfy the relation

$$\eta_{st} + \eta_{ol} + \eta_{cx} + \eta_{bh} = 1 \tag{6}$$

which is the energy conservation relation.

The radial electric field in the stationary state is determined by the charge neutrality equation. We solve the equation

$$\Gamma_{NC}{}^{e} = \Gamma_{NC}{}^{i} + \Gamma_{lc} + \Gamma_{cx} \tag{7}$$

to determine the radial electric field profile $E_r(r)$. The suffix NC indicates the neoclassical contribution, lc for loss cone and cx for the charge exchange loss, respectively. The superscript e and i denote electrons and ions, respectively. The expression of the neoclassical transport we employ here is quoted from Ref.[5]. The form of the current driven by the charge exchange loss is given as[16]

$$\Gamma_{cx} = (c/eB_p)M_f n_f n_0 \langle \sigma v_b \rangle v_{ft} \tag{8}$$

where B_p is the poloidal magnetic field, M_f is the mass of fast ions, n_0 is the neutral particle density, n_f is the fast particle density, v_b is the beam velocity $\sqrt{2W_b/M_f}$, v_{ft} is the toroidal velocity of the fast ions, and σ is the charge-exchange cross section which can be approximately given as [22]

$$\sigma = \frac{0.6937 \times 10^{-18}(1 - 0.155\ log_{10}E_b)^2}{1 + 0.1112 \times 10^{-14}E_b^{3.3}}[m^2], \tag{9}$$

Equation (7) is solved with the boundary condition that

$$E_r \rightarrow 0 \text{ as } r \rightarrow 0. \tag{10}$$

It is noted that the solution of Eq.(7), $E_r(r)$, is a functional of the parameter r_*, because the loss cone current Eq.(4) depends on the choice of r_*. We have the equation (2), which r_* must satisfy. The radial $E_r(r)$ and the eigenvalue r_* are determined to satisfy Eqs.(2) and (7). Thus we can determine the radial electric field and the loss rate simultaneously.

§3 Application to the NBI Heated Plasma

3.1 Determination of the Radial Electric Field

We first show the selfconsistent solution of $E_r(r)$ for the given profiles of plasma density and temperature. As a first step the contribution of the neutral particle is neglected.

Numerical example is obtained. Figure 2 shows the sample distributions of density and temperatures. The profiles are assumed as, simulating results in Ref.[8],

$$N(\rho) = [n(0)-n_s](1-\rho^{\alpha_2})^{\beta_2} + n_s, \tag{11}$$

$$T_e(\rho) = [T_e(0)-T_{es}](1-\rho^{\alpha_3})^{\beta_3} + T_{es}, \tag{12}$$

and

$$T_i(\rho) = [T_i(0)-T_{is}](1-\rho^{\alpha_4})^{\beta_4} + T_{is}, \tag{13}$$

where ρ is the normalized minor radius $\rho=r/a$, and the indices (α_k, β_k) are constant (k=2-4). n_s and T_s represents the values at plasma edge. For the present analysis, we choose the parameters of the shape as $\alpha_2=5$, $\beta_2=7$, $\alpha_3=7$, $\beta_3=7$, $\alpha_4=8$, $\beta_4=42$. Plasma parameters are $n_{e0}=6.8\times10^{19}/m^3$, $T_{e0}=350eV$, $T_{i0}=530eV$. No impurity ions are taken into account. The injection power is taken to be 1.2MW.

Based on a thin pencil beam model of the injected fast neutral particles we calculate the birth profile. This simplification allows us to use

$$P(x)/P(a) = \exp\{-\int_x^a \xi(x)[du/dx]dx\} \tag{14}$$

where the integral is taken along the path u, $x = u\cos\theta_{inj}$, θ_{inj} is the injection angle of the neutral beam with respect to the magnetic axis and the rate of the ionization ξ is approximated as

$$\xi = n_e\langle\sigma\rangle. \tag{15}$$

This is because the fast neutrals first exchange electrons with slow plasma ions and then ionized by electrons for the parameter of our interest. The direct ionization of fast neutral particles by electrons enhances ξ slightly, but this does not change the following conclusion. [One can use more correct form of P(r) if necessary.] The following calculations were done by taking b=a.

Figure 3 shows the dependence of each current component on E_r at ρ=0.8. Solid line indicates the electron current, which has a very weak dependence on E_r. The dashed lines indicate Γ^i in the absence of direct orbit loss (r_*=a), the case of r_*/a =0.5 and 0.3, respectively. If the loss boundary approaches to the axis, the loss current increases and the radial electric field becomes more negative. This graph shows that the influence of the ion orbit loss is large, so that the self consistent determination is inevitable.

We also note that a simple multiplication of $\Gamma_{NC}{}^i$ is not effective in increasing the radial electric field. We see that $\partial\Gamma_{NC}/\partial E_r$ is large for ions compared to electrons, and the absolute value of Γ_{NC}^{e} is small. The electric field is close to the value E_{r0} which is given by the relation

$$\Gamma_{NC}^{i}[E_{r0}] = 0. \tag{16}$$

The solution E_{r0} is not influenced by multiplying the constant factor on Γ_{NC}^{i}. The enhancement by the factor 10 to the neoclassical estimation does not give a noticeable difference in the solution of Eq.(7).

By determining the loss boundary self-consistently, we have the radial profile of the electric field in Fig.4. We take W_b as 14keV. (Half of the nominal injection energy is chosen as an average. This is because the power partition between the injection energy and 1/2 and 1/3 energies W_b, $W_b/2$, and $W_b/3$ is 4:3:3.) The loss boundary is calculated as

$$r_* = 0.5\ a$$

for this case. The radial profile in the region of $r<a/2$ is determined by the neoclassical process. The partition of the injection power is given as

$$\eta_{st} : \eta_{ol} : \eta_{bh} = 0.49 : 0.04 : 0.47. \tag{17}$$

About 10% of the born particles is lost as the direct orbit loss.

The enhancement of radial electric field is found in the peripheral region, which is effective in confining about 1/2 of the injected fast ions.

We study the effect of the birth profile on the radial electric field and loss cone boundary. In a preceding article, we have chosen a simple uniform profile. In this case the loss rate is larger as $\eta_{ol}:\eta_{bh}=3:7$, and the boundary was given $r_*/a=0.67$. In this paper, the birth profile is larger near the axis due to the peaked density profile. The loss boundary approaches to the axis, since the birth particles are small near the boundary.

Figure 5 illustrates the dependence on the injection energy. As the injection energy increases, the loss boundary invades into the plasma axis, and the loss rate increases. The radial electric field near the plasma boundary as well as the potential difference between the plasma surface and the loss boundary r_*, $\Phi(a)-\Phi(r_*)$, increase, which are necessary to confine fast ions. The radial electric field at r=0.8a and $\Phi(a)-\Phi(r_*)$ are illustrated as a function of the injection energy in Fig.6. In a high energy limit, the radial electric field approaches to the value

$$E_r = -W_b/eR \qquad (18)$$

which indicates the necessary radial electric field which cancels the ∇B drift.

The radial profile of the power flux and the normalized loss cone current are shown in Fig.7 for the cases of W_b=24keV, 14keV and 9keV. The ratio of the power partition is given as

$$\eta_{st} : \eta_{ol} : \eta_{bh} = 0.58 : 0.12 : 0.30. \quad (W_b=24\text{keV}) \tag{19-1}$$

$$\eta_{st} : \eta_{ol} : \eta_{bh} = 0.49 : 0.04 : 0.47. \quad (W_b=14\text{keV}) \tag{19-2}$$

$$\eta_{st} : \eta_{ol} : \eta_{bh} = 0.37 : 0.02 : 0.61. \quad (W_b=9\text{keV}) \tag{19-3}$$

The bulk heating is effective for the low injection energy (W_b=9keV), but is not effective in case of the high energy (W_b=24keV). If the injection energy becomes high, the ratio of the direct loss with respect to the ionized particles increases rapidly. In the case of W_b=24keV, this ratio is about 30%. This value is in a range of experimental observations[13].

3.2 Influence of Neutral Particles

The important role of neutral particles in determining the radial electric field has been discussed literature[16,18,19]. We here examine the effect of the neutral particles on the radial electric field.

The contribution of the radial current is given in Eq.(7). We choose a model distribution for fast particles and neutral particles as

$$n_f = n_{f0} \exp\{-\alpha_f \rho^2\} \tag{20}$$

and

$$n_0 = n_{0s}\ \exp\{-\alpha_0(1-\rho)^2\} \qquad (21)$$

where n_{f0} is the fast ion density at the center, n_{0s} is the neutral particle density at edge. Parameters α_f and α_0 are assumed to be constant. As a model case, we take the shaping parameter as $\alpha_f=2$ and $\alpha_0=40$, modelling the broad fast ion profile and localization of the neutrals near the edge. We also choose an example of $W_b=14$keV, and the nearly perpendicular injection where the injection angle $\theta_{inj}=\pi/30$ is taken. v_{ft}, which is estimated by $v_b \sin\theta_{inj}$, is then 1/10 of the injection velocity v_b.

Figure 8 illustrates the radial electric field in the presence of neutral particle contributions. We have chosen the parameter $n_{f0}=10^{18}/m^3$. Neutral particle density is varied as $n_{0s}=1\times$ and $2.5\times 10^{16}/m^3$. We see that the radial electric field becomes more negative near the plasma edge.

Associated with this increment of the radial electric field, the direct orbit loss is reduced. Figure 9(a) shows the loss cone boundary and the potential difference between the surface and loss cone boundary, $\Phi(a)-\Phi(r_*)$, as a function of the neutral particle density. Figure 9(b) shows the loss cone flux $\Gamma(x)_{lc}$. The enhanced radial electric field is effective in narrowing the loss cone. It is noted, however, that this does not mean that the total loss of fast ions is reduced. In case of $n_{0s}=2.5\times 10^{16}/m^3$ and the assumption of the profiles of n_f and n_0, the cx loss of fast ions reaches about 190kW. If we compare the partition between the shine through, direct orbit loss, cx loss of fast particles and bulk heating, we have

$$\eta_{st}:\eta_{ol}:\eta_{cx}:\eta_{bh} = 0.49 : 0.04 : 0.0 : 0.47 \qquad (21)$$

in the absence of neutral particles (line (1) in Fig.9(b)), but

$$\eta_{st}:\eta_{ol}:\eta_{cx}:\eta_{bh} = 0.49 : 0.015 : 0.15 : 0.35 \qquad (21)$$

in the presence of neutral particles (line (3) in Fig.9(b)). The ratio of the orbit loss is reduced, but the increment of the cx loss is much larger than this reduction.

3.3 Effect on the Bulk Energy Transport

It is often discussed that the enhanced electric field can reduce the energy and particle loss. We study the influence of the energetic particle loss on the neoclassical flux of bulk particles.

Using the obtained radial electric field profile $E_r(r)$ with the density and temperature profiles, the particle and energy fluxes are calculated according to the formula of Ref.[5].

Figure 10 shows the neoclassical particle flux for the cases of radial electric field with (a) no fast ion loss (b) direct orbit loss and (c) direct loss and cx loss. As is seen from Fig.3, the particle flux becomes larger if the radial electric field becomes more negative. By this mechanism, the net particle flux increases due to the fast particle loss. The loss flux governed by the neoclassical process, however, is small, so that the increment of the particle flux does not give rise to a considerable harm to the confinement.

The neoclassical energy flux of electrons and ions are shown in Fig.11. We see that the ion energy flux decreases by the fast particle effect. The electron energy flux, on the other hand, increases by the negative radial electric field. The ion energy loss is dominant over the electron loss near the half radius of the plasma core. The radial electric field in this region, however, is determined by the bulk radial current, and is not influenced by the fast particles. Table 1 summarizes the trade off concerning on the energy balance.

Table 1 shows the neoclassical energy flux of bulk ions $q_{NC}{}^{i}$, which is calculated using the radial electric field in which the fast ion loss is neglected, and that calculated with the electric field keeping fast ion loss, $q_{NC+orbit}$. The reduction of the neoclassical ion energy flux

$$\Delta q^{i} = q_{NC}{}^{i} - q_{NC+orbit}{}^{i}$$

is caused by the enhancement of the radial electric field by the fast ions. The fourth column indicates the loss flux of fast ions. These quantities are tabled for various magnetic surfaces. Injection energy takes the values W_b=14keV and 24keV. In all cases, the power loss of fast ions are greater than the reduction of the bulk ion loss by a factor of several tens to 100. This clearly shows that the enhancement of the radial electric field by using the fast ion loss is not useful so long as one considers the neoclassical energy loss.

§4 Summary and Discussion

We have developed a selfconsistent analysis in determining the radial electric field and ion loss cone. Analysis was applied to the Wendelstein VII-A stellarator. The solution of the radial electric field has one or two maxima and cannot be approximated by a simple parabolic model of the static potential. The increased loss makes the radial electric field deeper. The effect is prominent near the plasma boundary, and the experimental observation is better reproduced in comparison with the simple neoclassical analysis in which the fast particle loss is neglected. The loss rate of fast ions is evaluated as a function of the injection energy, and is found in the range of experimental observations. If one takes into account the charge exchange loss effect by neutrals, the electric field becomes more negative. The more precise experimental data would provide a test of the validity of the modelling.

The influence of the neutral particles on the direct orbit loss is also studied. The neutral particles, through the influence on the radial electric field, can affect the direct loss considerably. The total fast ion loss, which comes either from direct loss or cx loss, does not change drastically. However, the direct orbit loss alone can be reduced. The interaction of fast particles with the wall is different between the direct orbit loss and cx loss. The direct orbit loss is often localized at particular toroidal/poloidal position of the wall. On the other hand, the cx loss is more or less uniform so long as the neutral particles are not localized at special location. When the heat load onto the wall is analyzed, the partition between the direct loss and the cx loss through changing the radial electric field must be kept in considerations.

The increased electric field can reduce the neoclassical thermal conduction. The neoclassical component of the ion heat flux, which is derived using $E_r(r)$, reduces from 15kW (E_r without fast ion loss effect) to 14kW (in the case of W_b=14keV) at ρ=0.7. This reduction, which amounts to 1kW, however, is smaller than the increment in the direct orbit loss of about 40kW. From the over all consideration on the energy balance, if one uses the neoclassical estimate, it is concluded that the enhanced fast ion loss is energetically not favorable. The energy balance in a real experimental plasmas, however, is strongly influenced by the anomalous energy loss. The effect of this change of the radial electric field on the anomalous loss needs investigation, in order to conclude the over all trade-off on the energy balance. The role of this radial electric field on the anomalous transport is discussed in a separate article[23], but still needs further intense analysis.

Acknowledgements

One of the authors (KI) acknowledges discussions with Drs. H. Wobig, H. Zushi and K. Hanatani. This work is partly supported by the Grant in Aid for Scientific Research of the Ministry of Education, Japan.

References

[1] H. P. Furth and M. N. Rosenbluth: in Plasma Physics and Controlled Nuclear Fusion Research, Proceedings of the 3rd International Conference, 1968 (IAEA. Vienna, 1969) Vol.1, p.821.

[2] K. Miyamoto: Nucl. Fusion **18** (1978) 243.

[3] H. E. Mynick: Phys. Fluids **26** (1983) 1008.

[4] B. B. Kadomtsev, and O. P. Pogutse, Nucl. Fusion **11** (1971) 67.

[5] L. M. Kovrizhnykh: Nucl. Fusion **24** (1984) 435.

[6] D. E. Hastings: Phys. Fluids 27 (1984) 2372.

[7] For a review, see G. Grieger and W VII-A Team: Plasma Physics and Controlled Fusion **28** (1986) 43.

[8] H. Renner, W VII-A Team, NBI Group, ICF Group, 'Overview on recent W VII-A experimental Results' in Proc. 6th International Stellarator/Heliotron Workshop (IAEA Tech Committee Meeting, Kyoto, 1986) Vol.1, p23.

[9] W VII-A Team and NI Team: in Proc. 11th European Conference on Controlled Fusion and Plasma Physics (Aachen, 1983) Vol.7D Part I, 199.

[10] S.-I. Itoh and K. Itoh: Phys. Rev. Lett.**60** (1988) 2276.

[11] R. J. Groebner, P. Gohil, K. H. Burrell, et al: Phys. Rev. Lett. **64** (1990) 3015.

[12] K. Ida, S. Hidekuma, Y. Miura, et al: Phys. Rev. Lett. **65** (1990) 1364.

[13] W VII-A Team and NI Team (presented by J. Junker): 'Ion Heating and Orbit Losses in NI Experiments on Wendelstein

VII-A' in Proc. 5th International Workshop on Stellarators (IAEA Tech. Committee Meeting, Schloss Ringberg, 1984) Vol.1, p179.

[14] K. Hanatani, private communications

[15] K. Watanabe, Y. Nakamura and M. Wakatani: J. Phys. Soc. Jpn. **60** (1991) 884.

[16] H. Sanuki, K. Itoh, K. Ida and S.-I. Itoh: 'On Radial Electric Field in CHS Torsatron/Heliotron' Research Report NIFS-94 (National Institute for Fusion Science, 1991), submitted to J. Phys. Soc. Jpn. for publication.

[17] K. Itoh, H. Sanuki, S.-I. Itoh: 'Influence of Fast Ion Loss on Radial Electric Field in Wendelstein VII-A Stellarator', Research Report NIFS-95 (National Institute for Fusion Science, 1991).

[18] T. Ohkawa: Kakuyuugou Kenkyuu **56** (1986) 274.

[19] K. C. Shaing: Comments on Plasma Physics and Controlled Fusion **12** (1988) 69.

[20] G. I. Budker, in Plasma Physics and the Problem of Controlled Thermonuclear Reactions (ed., M. A. Leontovich, Pergamon Press, Inc., New York, 1961) Vol.1, p78.

[21] K. Itoh, H. Sanuki, J. Todoroki, et al: Phys. Fluids **B3** (1991) 1294.

[22] A. C. Riviere: Nucl. Fusion **11** (1971) 363.

[23] K. Itoh, et al: "H-mode like bifurcations of the Core Plasma in Stellarators" Research Report NIFS-97 (National Institute for Fusion Science, 1991).

Figure Captions

Fig.1 Schematic plot of the drift surface of the fast ions and neutral beam(a). r_* indicates the loss cone boundary. The current across the surface r=r associated with the loss cone is given by the particle source in the region $[-r, -r_*]$. Beam power density P, birth profile S and the loss cone current are shown schematically in (b).

Fig.2 Density (a) and temperature (b) profiles for the analysis. (α_2=5, β_2=7, α_3=7, β_3=7, α_4=8, β_4=42.) Central electron density is given as $6.8\times10^{19}/m^3$.

Fig.3 Dependences of the current component on the radial electric field on the minor radius of ρ=0.8. Solid line is for electron component. Ion current by the neoclassical prediction (dotted line), that with the ion orbit loss (cases of ρ_* = 0.3 and 0.5; dashed lines) and that estimated by 10 times of neoclassical flux (dashed-dotted line) are shown. Circles indicate the solution of of the radial electric field. Injection energy is 14keV and the power is 1.2MW.

Fig.4 Radial profile of the radial electric field. Solid line is the selfconsistent solution for the electric field and fast ion loss. Line with (1) indicates the case of W_b=14keV and that with (2) is for W_b=28keV. Dotted line is for the neoclassical prediction. It is noted that the influence of the ion orbit loss is substantial near the plasma edge. For the case of W_b=14keV (line (1)), the loss cone boundary is given as ρ_*=0.5, but the deviation of E_r from the neoclassical prediction becomes noticeable for ρ>0.7. Solid circles indicate experimental results (quoted from Ref.[8]).

Fig.5 Dependence of the loss cone boundary on the injection energy. Injection power is kept 1.2MW and other parameters are the same is in Fig.2.

Fig.6 The radial electric field at ρ=0.8 (solid line) and the potential difference between the surface and loss cone boundary (dashed line) as a function of the injection energy. (dotted line shows the result of neoclassical calculation without fast ion loss for the reference.) Thin dashed-dotted line indicates W_b/eR. Injection power is kept 1.2MW and other parameters are the same is in Fig.2.

Fig.7 Normalized distributions of the power flux of the neutral beam (solid lines) and the loss cone current. (a), (b), and (c) indicate W_b=24keV, 14keV and 9keV, respectively.

Fig. 8 Effect of the cx loss on radial electric field. Solid lines are the selfconsistent solution for the electric field and fast ion loss. Dotted line is for the neoclassical prediction. (1), (2) and (3) corresponds to cases $n_{0s}=0$, $10^{16}/m^3$ and $2.5\times10^{16}/m^3$. Solid circles indicate experimental results (quoted from Ref.[8]).

Fig. 9 The loss cone boundary ρ_* (solid line) and the potential difference between the surface and loss cone boundary (dashed line) as a function of the neutral particle density (a). Normalized distributions of the power flux of the neutral beam (solid lines) and the loss cone current.(b). In (b), (1), (2), and (3) indicate cases $n_{0s}=0$, $10^{16}/m^3$ and $2.5\times10^{16}/m^3$, respectively. Injection energy is kept 14keV, the injection power is kept 1.2MW and other parameters are the same is in Fig. 2.

Fig. 10 Particle flux profile in the case of (a) simple neoclassical prediction, (b) with direct orbit loss and (c) with direct ion loss and cx loss, respectively. In (c), $n_{0s}=5\times10^{16}/m^3$. $W_b=14$keV and other parameters are the same as in Fig. 3.

Fig. 11 Electron energy flux (a) and ion energy flux (b).

Symbols (a), (b) and (c) correspond to those in Fig.10.

ρ	W_b keV	$q_{NC}{}^{i}$ [kW]	$q_{NC+orbit}{}^{i}$ [kW]	Δq^{i} [kW]	P_{loss} [kW]
0.60	14	193.4	192.0	1.4	24.0
	24	〃	189.0	4.4	128.4
0.65	14	79.4	78.2	1.2	30.0
	24	〃	76.5	2.9	132.0
0.70	14	14.8	14.0	0.8	38.4
	24	〃	13.1	1.7	141.6
0.75	14	1.7	1.1	0.6	43.2
	24	〃	0.6	1.1	144.0

Table 1 Energy fluxes at various radius (ρ=0.6, 0.65, 0.7 and 0.75) for two injection energy W_b=14keV and 24keV. Radial electric field is given by the simple neoclassical theory ($\Gamma_{NC}{}^{e}=\Gamma_{NC}{}^{i}$) in calculating q_{NC}. Orbit loss is taken into account in estimation radial electric field ($\Gamma_{NC}{}^{e}=\Gamma_{NC}{}^{i}+\Gamma_{lc}{}^{i}$) in calculating $q_{NC+orbit}$. Δq is defined by $q_{NC}-q_{NC+orbit}$.

Fig. 1

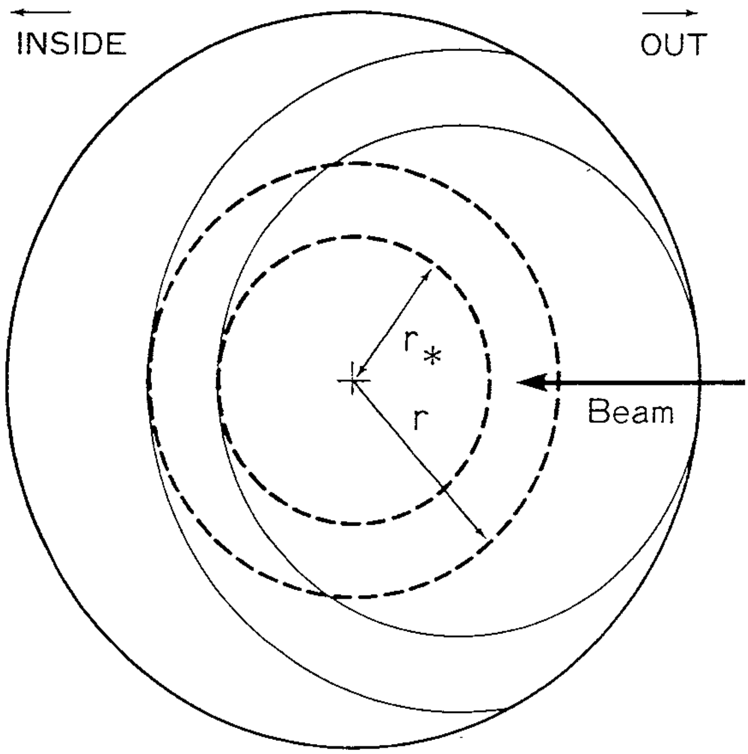

(a)

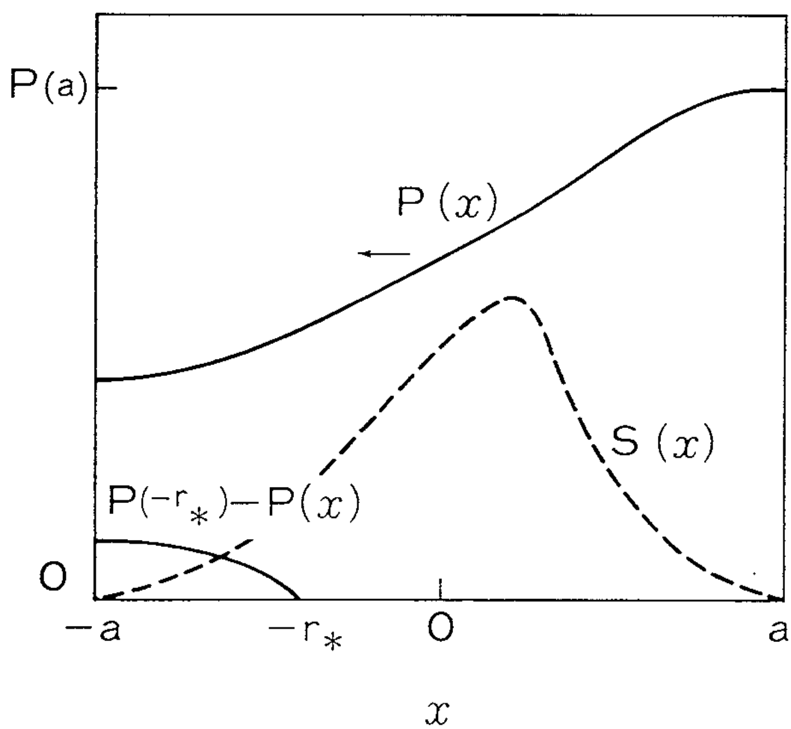

(b)

Fig. 2

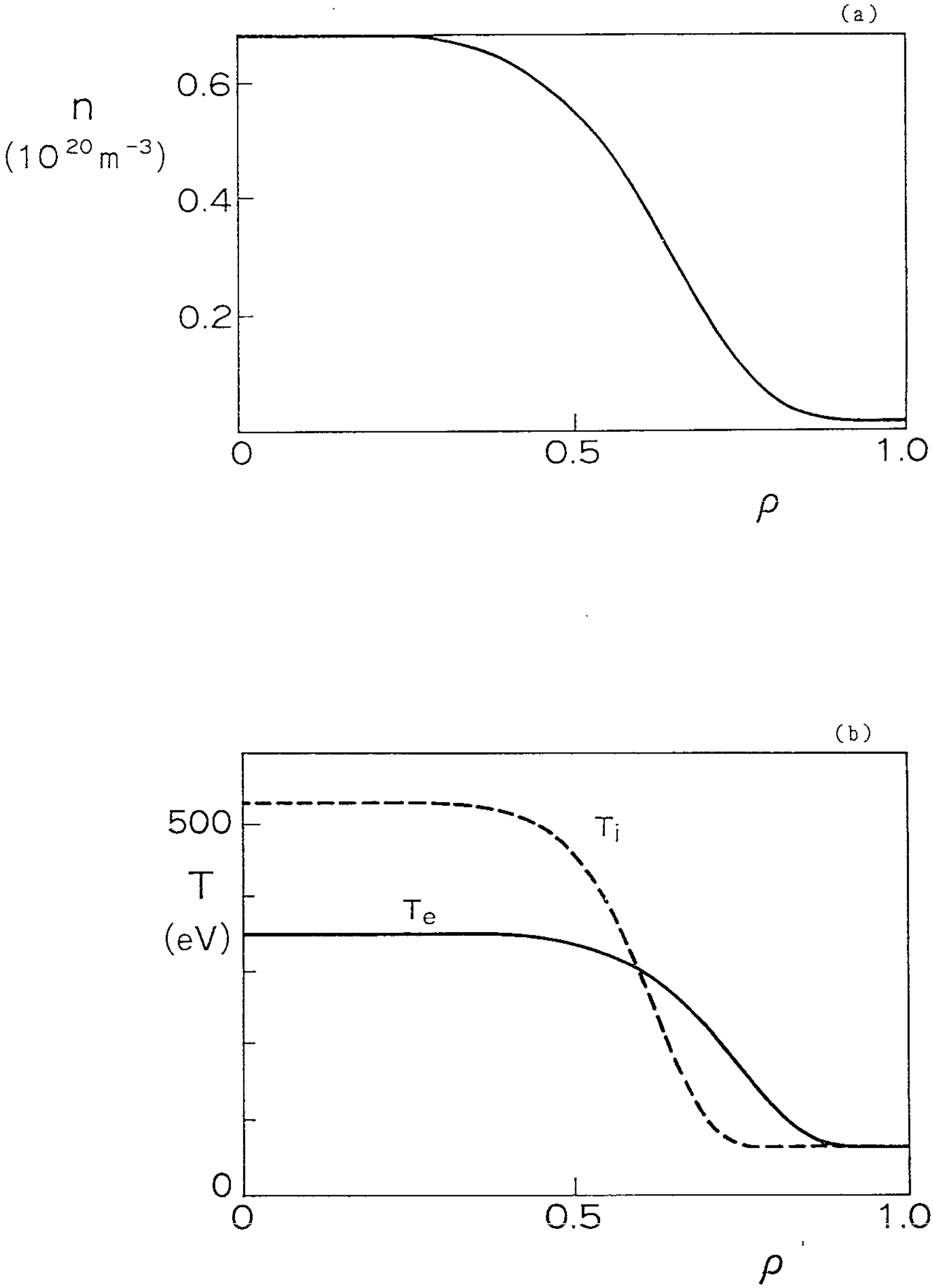

Fig.3

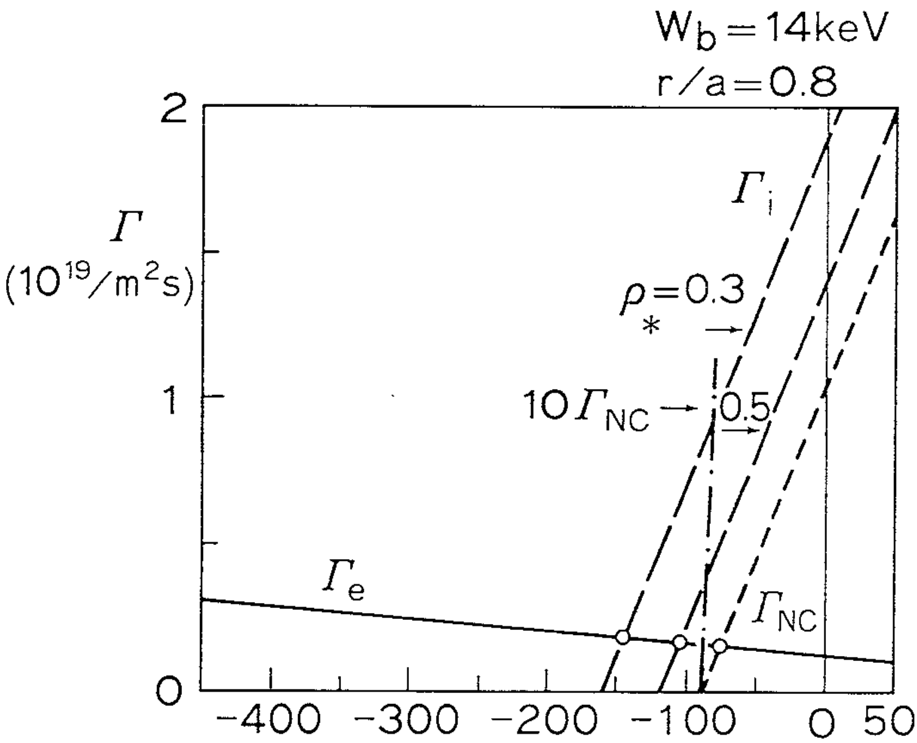

W_b = 14keV
r/a = 0.8
2
Γ
(10^19/m^2s)
1
0
Γ_i
ρ_* = 0.3
10Γ_NC
0.5
Γ_e
Γ_NC
-400 -300 -200 -100 0 50
E_r (V/cm)

Fig. 4

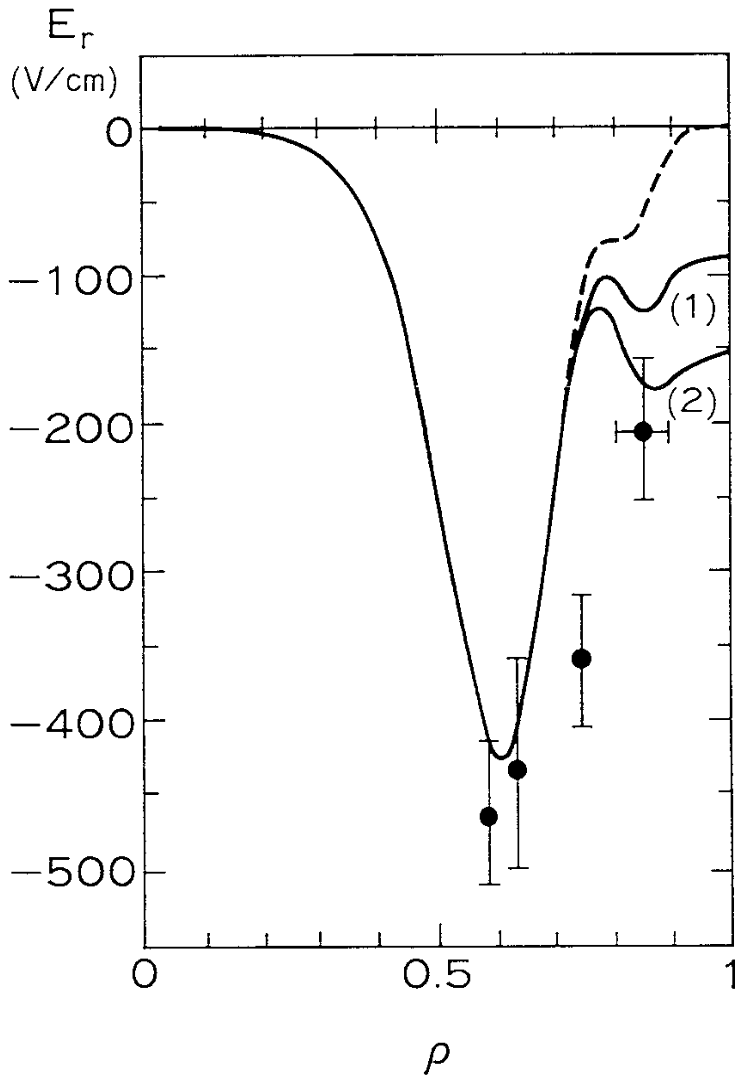

Fig. 5

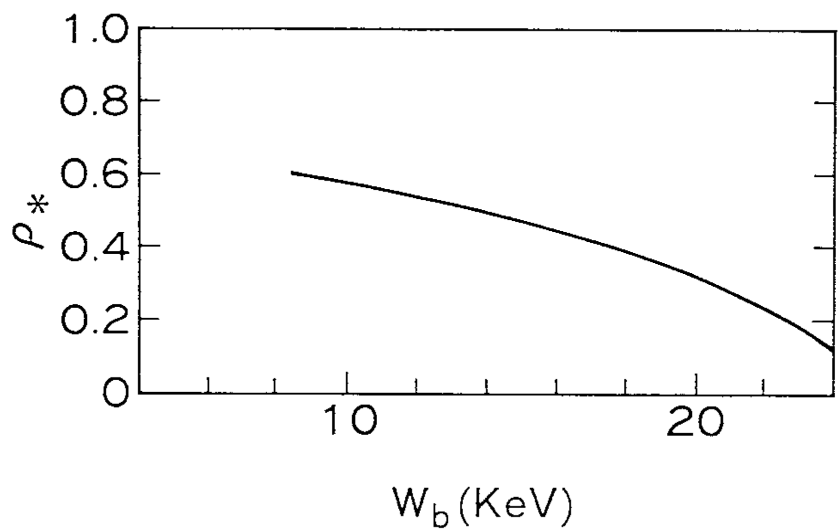

Fig. 6

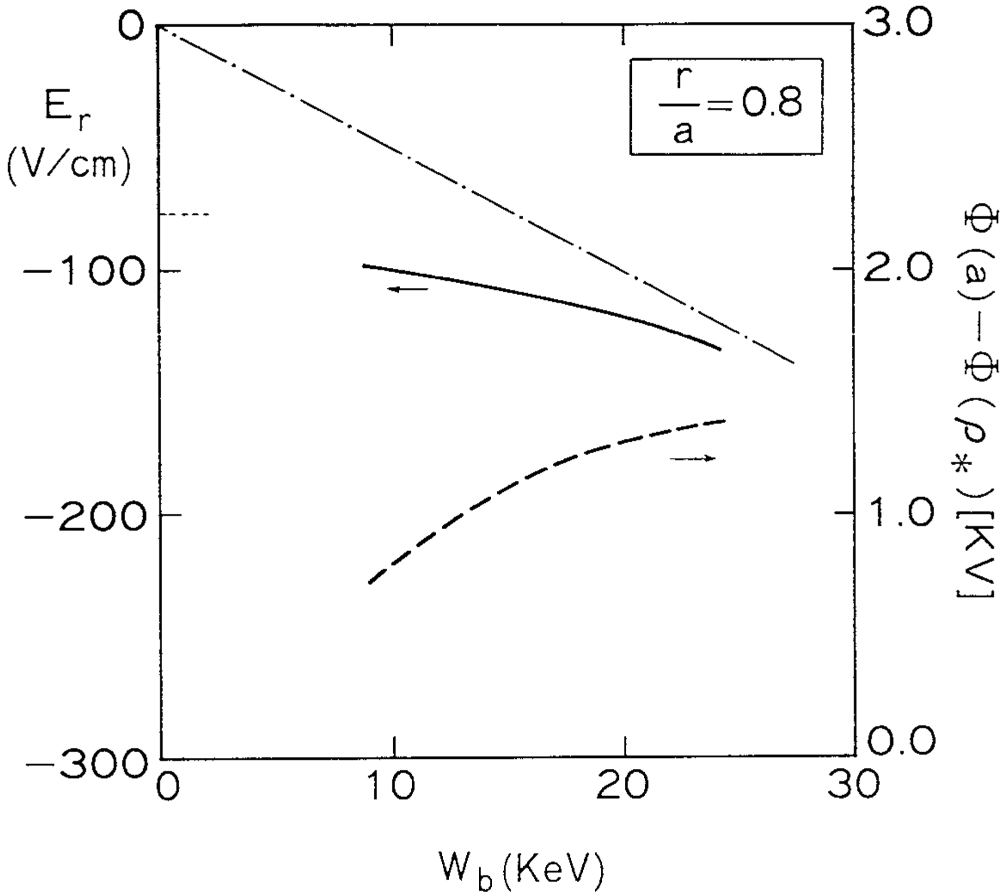

0
-100
-200
-300
E_r (V/cm)
3.0
2.0
1.0
0.0
$\Phi(a) - \Phi(\rho_*)$ [KV]
$\frac{r}{a} = 0.8$
0
10
20
30
W_b (KeV)

Fig. 7

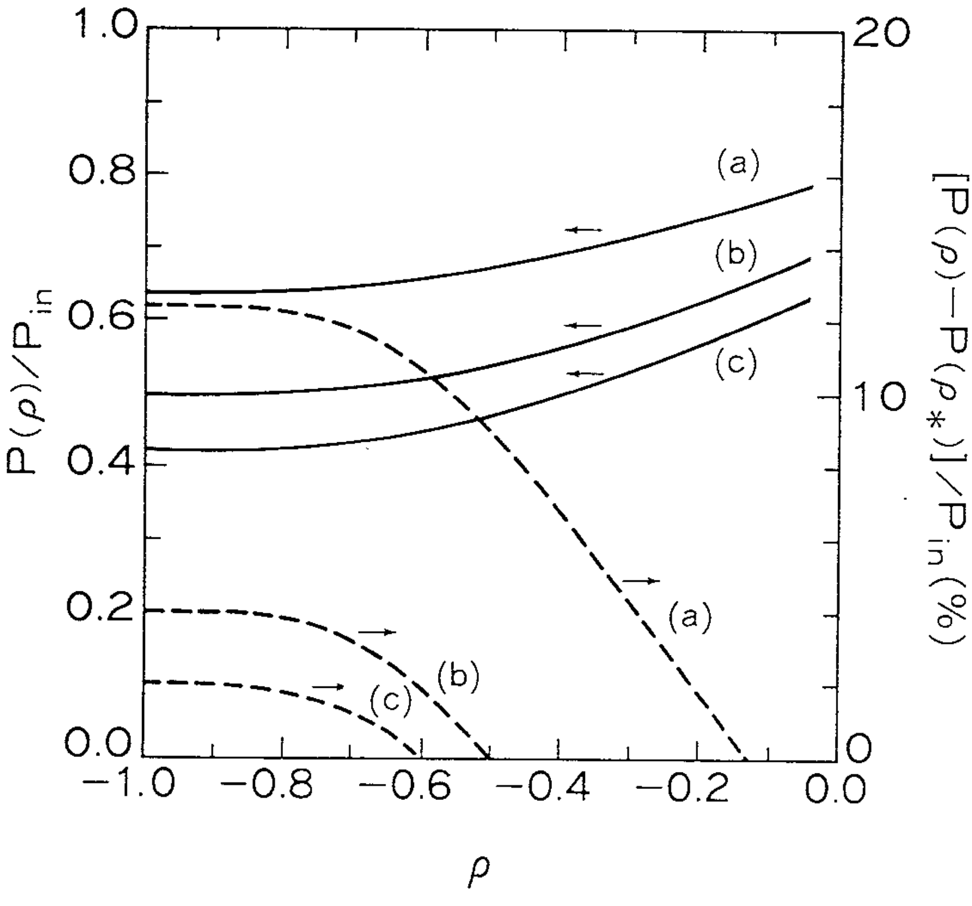

Fig. 8

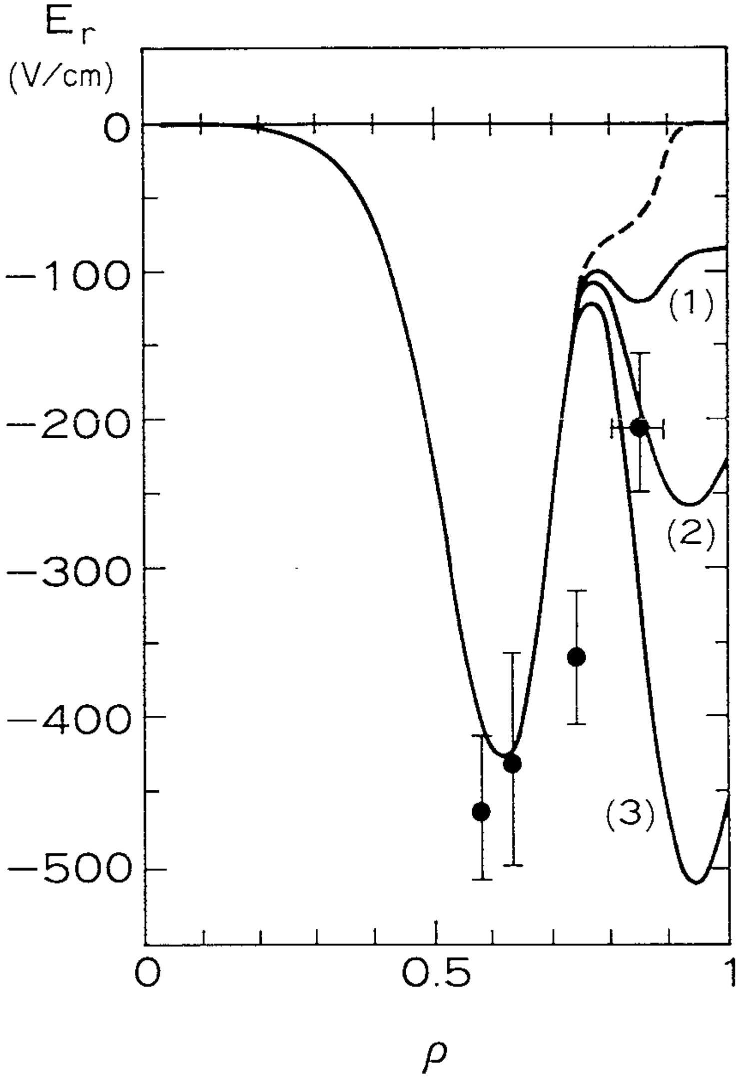

Fig. 9(a)

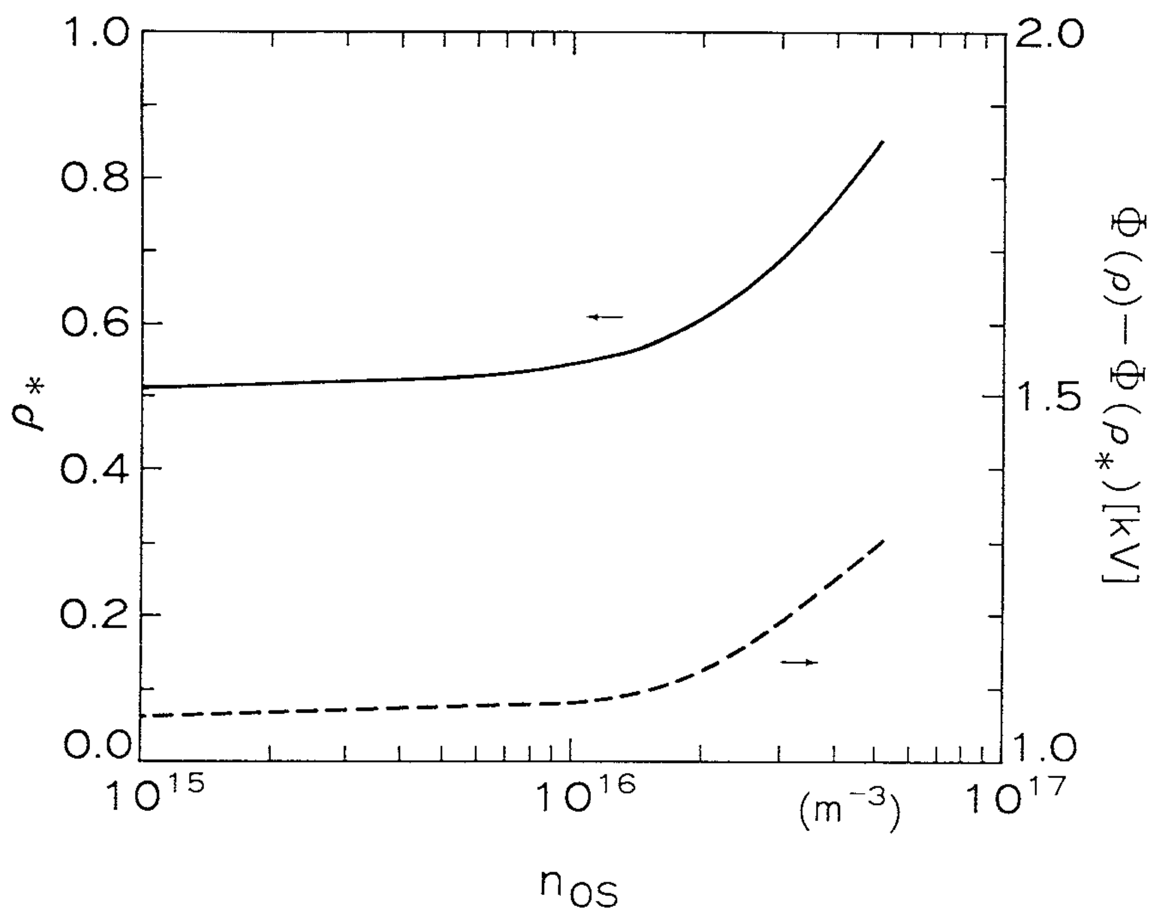
1.0
0.8
0.6
0.4
0.2
0.0
2.0
1.5
1.0
ρ_*
$\Phi(\rho)-\Phi(\rho_*)$ [kV]
10^{15}
10^{16}
10^{17}
(m^{-3})
n_{os}

Fig. 9(b)

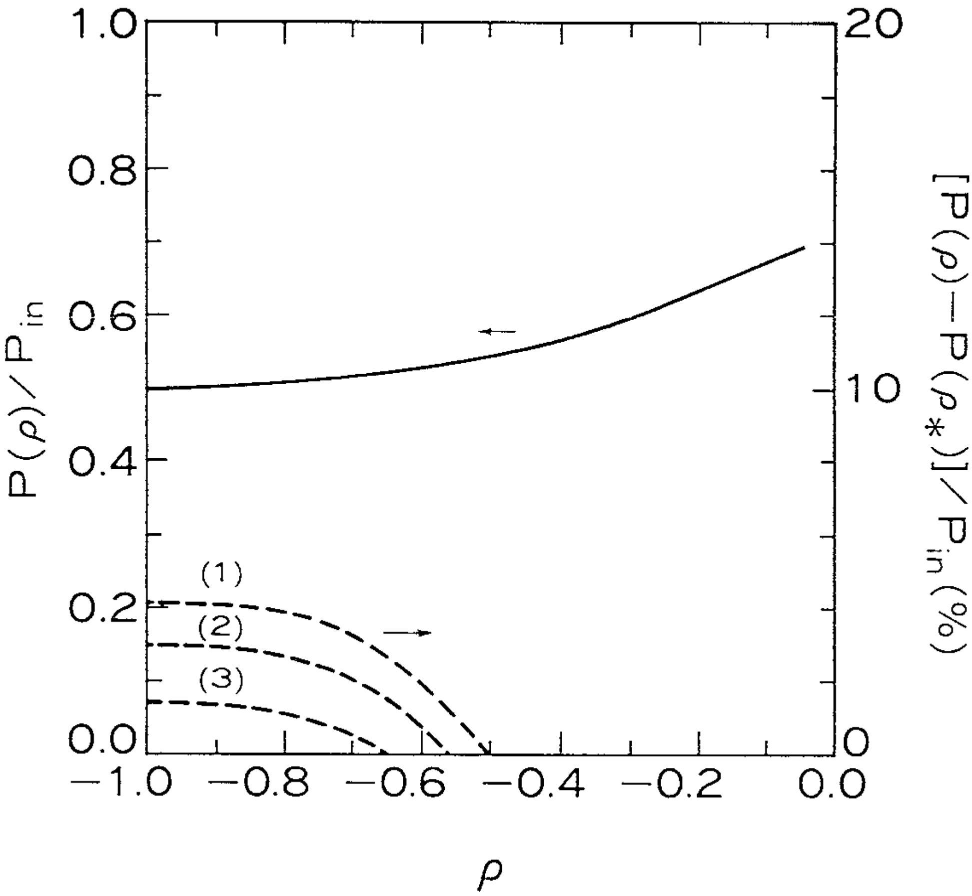

1.0
0.8
0.6
0.4
0.2
0.0
$P(\rho)/P_{in}$
20
10
0
$[P(\rho)-P(\rho_*)]/P_{in}$ (%)
(1)
(2)
(3)
−1.0
−0.8
−0.6
−0.4
−0.2
0.0
ρ

Fig.10

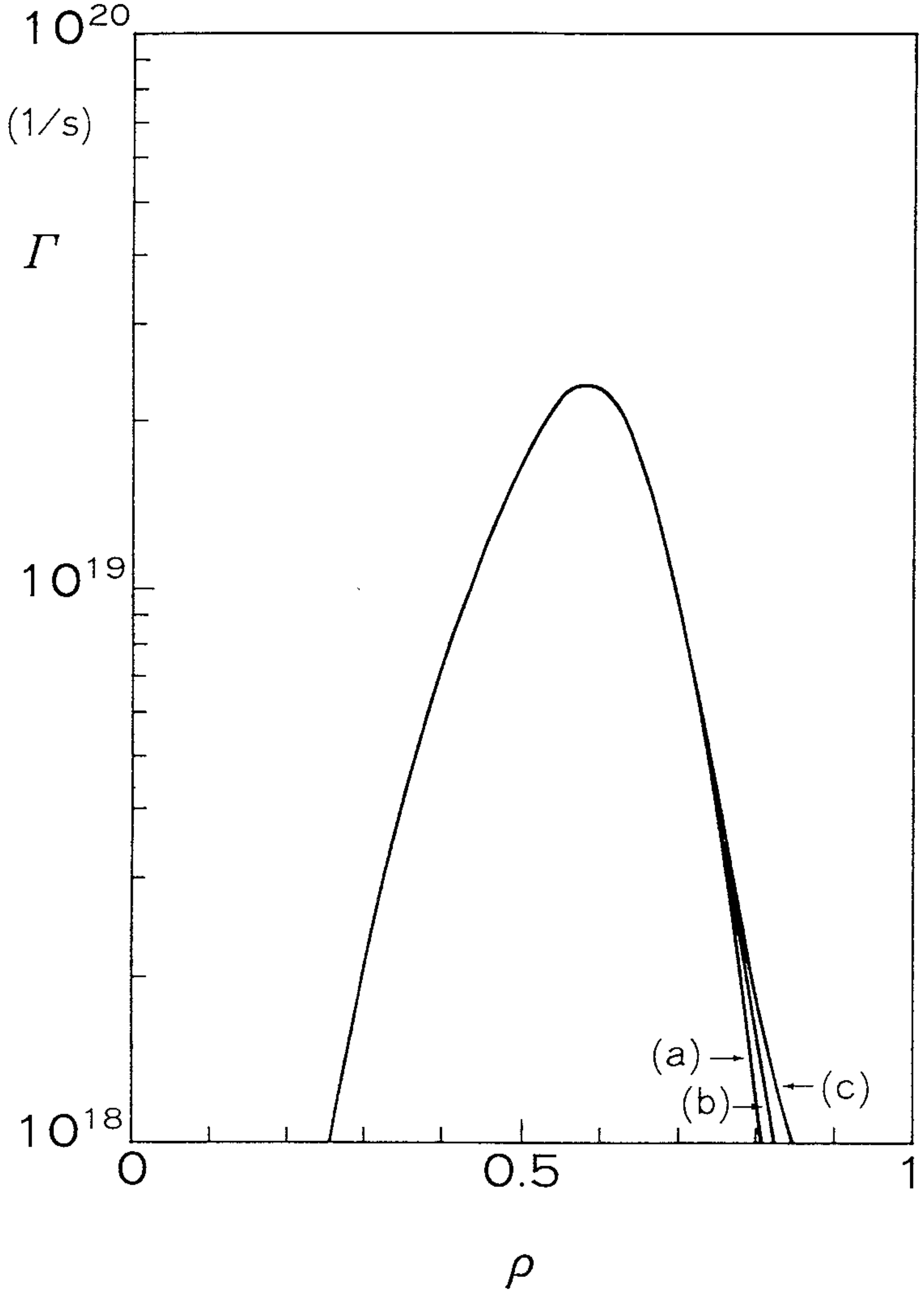

Fig. 11(a)

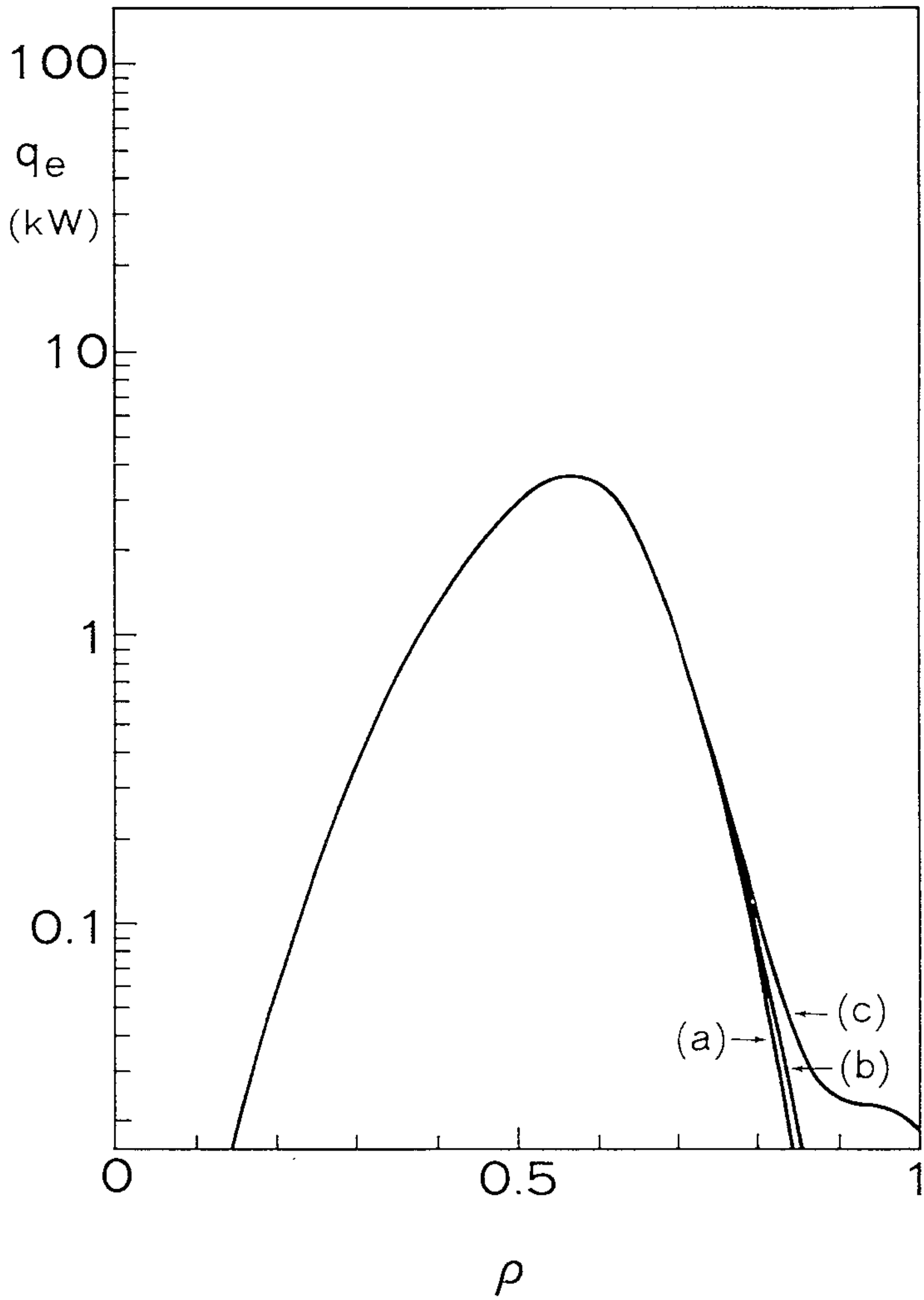

Fig. 11(b)

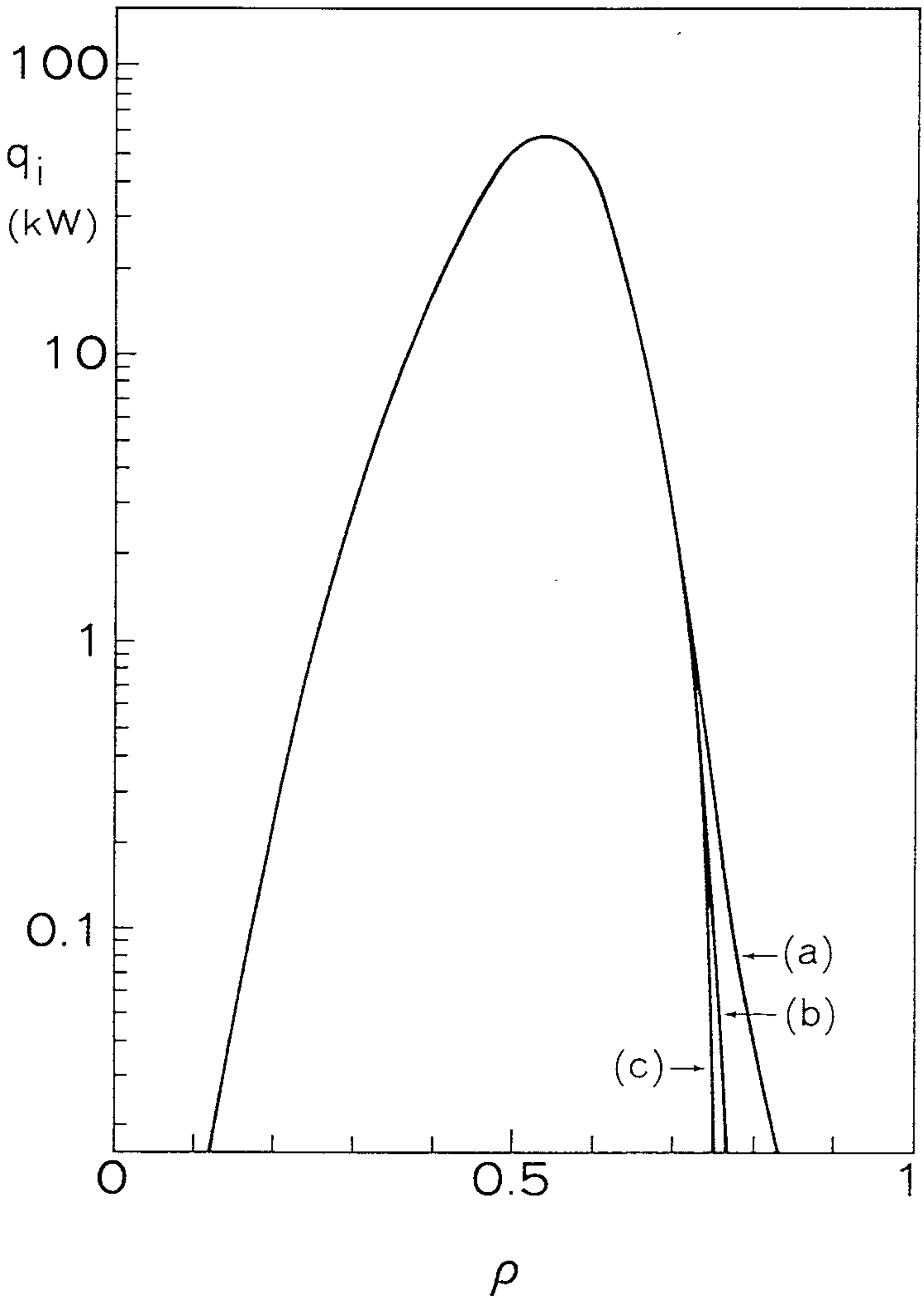

Recent Issues of NIFS Series

NIFS-57 S.-I.Itoh, H.Maeda and Y.Miura, *Improved Modes and the Evaluation of Confinement Improvement*; Oct. 1990

NIFS-58 H.Maeda and S.-I.Itoh, *The Significance of Medium- or Small-size Devices in Fusion Research*; Oct. 1990

NIFS-59 A.Fukuyama, S.-I.Itoh, K.Itoh, K.Hamamatsu, V.S.Chan, S.C.Chiu, R.L.Miller and T.Ohkawa, *Nonresonant Current Drive by RF Helicity Injection*; Oct. 1990

NIFS-60 K.Ida, H.Yamada, H.Iguchi, S.Hidekuma, H.Sanuki, K.Yamazaki and CHS Group, *Electric Field Profile of CHS Heliotron/Torsatron Plasma with Tangential Neutral Beam Injection*; Oct. 1990

NIFS-61 T.Yabe and H.Hoshino, *Two- and Three-Dimensional Behavior of Rayleigh-Taylor and Kelvin-Helmholz Instabilities*; Oct. 1990

NIFS-62 H.B. Stewart, *Application of Fixed Point Theory to Chaotic Attractors of Forced Oscillators;* Nov. 1990

NIFS-63 K.Konn., M.Mituhashi, Yoshi H.Ichikawa,*Soliton on Thin Vortex Filament;* Dec. 1990

NIFS-64 K.Itoh, S.-I.Itoh and A.Fukuyama,*Impact of Improved Confinement on Fusion Research;* Dec. 1990

NIFS -65 A.Fukuyama, S.-I.Itoh and K. Itoh,*A Consistency Analysis on the Tokamak Reactor Plasmas;* Dec. 1990

NIFS-66 K.Itoh, H. Sanuki, S.-I. Itoh and K. Tani,*Effect of Radial Electric Field on α-Particle Loss in Tokamaks;* Dec. 1990

NIFS-67 K.Sato,and F.Miyawaki,*Effects of a Nonuniform Open Magnetic Field on the Plasma Presheath*; Jan.1991

NIFS-68 K.Itoh and S.-I.Itoh,*On Relation between Local Transport Coefficient and Global Confinement Scaling Law;* Jan. 1991

NIFS-69 T.Kato, K.Masai, T.Fujimoto,F.Koike, E.Källne, E.S.Marmar and J.E.Rice,*He-like Spectra Through Charge Exchange Processes in Tokamak Plasmas;* Jan.1991

NIFS-70 K. Ida, H. Yamada, H. Iguchi, K. Itoh and CHS Group, *Observation of Parallel Viscosity in the CHS Heliotron/Torsatron* ; Jan.1991

NIFS-71 H. Kaneko, *Spectral Analysis of the Heliotron Field with the Toroidal Harmonic Function in a Study of the Structure of Built-in Divertor* ; Jan. 1991

NIFS-72 S. -I. Itoh, H. Sanuki and K. Itoh, *Effect of Electric Field Inhomogeneities on Drift Wave Instabilities and Anomalous Transport* ; Jan. 1991

NIFS-73 Y.Nomura, Yoshi.H.Ichikawa and W.Horton, *Stabilities of Regular Motion in the Relativistic Standard Map*; Feb. 1991

NIFS-74 T.Yamagishi, *Electrostatic Drift Mode in Toroidal Plasma with Minority Energetic Particles,* Feb. 1991

NIFS-75 T.Yamagishi, *Effect of Energetic Particle Distribution on Bounce Resonance Excitation of the Ideal Ballooning Mode*, Feb. 1991

NIFS-76 T.Hayashi, A.Tadei, N.Ohyabu and T.Sato, *Suppression of Magnetic Surface Breading by Simple Extra Coils in Finite Beta Equilibrium of Helical System;* Feb. 1991

NIFS-77 N. Ohyabu, *High Temperature Divertor Plasma Operation*; Feb. 1991

NIFS-78 K.Kusano, T. Tamano and T. Sato, *Simulation Study of Toroidal Phase-Locking Mechanism in Reversed-Field Pinch Plasma*; Feb. 199l

NIFS-79 K. Nagasaki, K. Itoh and S. -I. Itoh, *Model of Divertor Biasing and Control of Scrape-off Layer and Divertor Plasmas*; Feb. 1991

NIFS-80 K. Nagasaki and K. Itoh, *Decay Process of a Magnetic Island by Forced Reconnection*; Mar. 1991

NIFS-81 K. Takahata, N. Yanagi, T. Mito, J. Yamamoto, O.Motojima and LHDDesign Group, K. Nakamoto, S. Mizukami, K. Kitamura, Y. Wachi, H. Shinohara, K. Yamamoto, M. Shibui, T. Uchida and K. Nakayama, *Design and Fabrication of Forced-Flow Coils as R&D Program for Large Helical Device*; Mar. 1991

NIFS-82 T. Aoki and T. Yabe, *Multi-dimensional Cubic Interpolation for ICF Hydrodynamics Simulation*; Apr. 1991

NIFS-83 K. Ida, S.-I. Itoh, K. Itoh, S. Hidekuma, Y. Miura, H. Kawashima, M. Mori, T. Matsuda, N. Suzuki, H. Tamai, T.Yamauchi and JFT-2M Group, *Density Peaking in the JFT-2M Tokamak Plasma with Counter Neutral Beam Injection* ; May 1991

NIFS-84 A. Iiyoshi, *Development of the Stellarator/Heliotron Research*; May 1991

NIFS-85 Y. Okabe, M. Sasao, H. Yamaoka, M. Wada and J. Fujita, *Dependence of Au^- Production upon the Target Work Function in a Plasma-Sputter-Type Negative Ion Source;* May 1991

NIFS-86 N. Nakajima and M. Okamoto, *Geometrical Effects of the Magnetic Field on the Neoclassical Flow, Current and Rotation in General Toroidal Systems*; May 1991

NIFS-87 S. -I. Itoh, K. Itoh, A. Fukuyama, Y. Miura and JFT-2M Group, *ELMy-H mode as Limit Cycle and Chaotic Oscillations in Tokamak Plasmas;* May 1991

NIFS-88 N.Matsunami and K.Kitoh, *High Resolution Spectroscopy of H^+ Energy Loss in Thin Carbon Film;* May 1991

NIFS-89 H. Sugama, N. Nakajima and M.Wakatani, *Nonlinear Behavior of Multiple-Helicity Resistive Interchange Modes near Marginally Stable States;* May 1991

NIFS-90 H. Hojo and T.Hatori, *Radial Transport Induced by Rotating RF Fields and Breakdown of Intrinsic Ambipolarity in a Magnetic Mirror*; May 1991

NIFS-91 M. Tanaka, S. Murakami, H. Takamaru and T.Sato, *Macroscale Implicit, Electromagnetic Particle Simulation of Inhomogeneous and Magnetized Plasmas in Multi-Dimensions;* May 1991

NIFS-92 S. - I. Itoh, *H-mode Physics, -Experimental Observations and Model Theories-, Lecture Notes, Spring College on Plasma Physics, May 27 - June 21 1991 at International Centre for Theoretical Physics (IAEA UNESCO) Trieste, Italy ;* Jun. 1991

NIFS-93 Y. Miura, K. Itoh, S. - I. Itoh, T. Takizuka, H. Tamai, T. Matsuda, N. Suzuki, M. Mori, H. Maeda and O. Kardaun, *Geometric Dependence of the Scaling Law on the Energy Confinement Time in H-mode Discharges;* Jun. 1991

NIFS-94 H. Sanuki, K. Itoh, K. Ida and S. - I. Itoh, *On Radial Electric Field Structure in CHS Torsatron / Heliotron;* Jun. 1991

NIFS-95 K. Itoh, H. Sanuki and S. - I. Itoh, *Influence of Fast Ion Loss on Radial Electric Field in Wendelstein VII-A Stellarator;* Jun. 1991

NIFS-96 S. - I. Itoh, K. Itoh, A. Fukuyama, *ELMy-H mode as Limit Cycle and Chaotic Oscillations in Tokamak Plasmas;* Jun. 1991

NIFS-97 K. Itoh, S. - I. Itoh, H. Sanuki, A. Fukuyama, *An H-mode-Like Bifurcation in Core Plasma of Stellarators;* Jun. 1991

NIFS-98 H. Hojo, T. Watanabe, M. Inutake, M. Ichimura and S. Miyoshi, *Axial Pressure Profile Effects on Flute Interchange Stability in the Tandem Mirror GAMMA 10;* Jun. 1991

NIFS-99 A. Usadi, A. Kageyama, K. Watanabe and T. Sato, *A Global Simulation of the Magnetosphere with a Long Tail : Southward and Northward IMF;* Jun. 1991

NIFS-100 H. Hojo, T. Ogawa and M. Kono, *Fluid Description of Ponderomotive Force Compatible with the Kinetic One in a Warm Plasma* ; July 1991

NIFS-101 H. Momota, A. Ishida, Y. Kohzaki, G. H. Miley, S. Ohi, M. Ohnishi K. Yoshikawa, K. Sato, L. C. Steinhauer, Y. Tomita and M. Tuszewski *Conceptual Design of D-^{3}He FRC Reactor "ARTEMIS"* ; July 1991

NIFS-102 N. Nakajima and M. Okamoto, *Rotations of Bulk Ions and Impurities in Non-Axisymmetric Toroidal Systems* ; July 1991

NIFS-103 A. J. Lichtenberg, K. Itoh, S. - I. Itoh and A. Fukuyama, *The Role of Stochasticity in Sawtooth Oscillation* ; Aug. 1991

NIFS-104 K. Yamazaki and T. Amano, *Plasma Transport Simulation Modeling for Helical Confinement Systems;* Aug. 1991

NIFS-105 T. Sato, T. Hayashi, K. Watanabe, R. Horiuchi, M. Tanaka, N. Sawairi and K. Kusano, *Role of Compressibility on Driven Magnetic Reconnection ;* Aug. 1991

NIFS-106 Qian Wen - Jia, Duan Yun - Bo, Wang Rong - Long and H. Narumi, *Electron Impact Excitation of Positive Ions - Partial Wave Approach in Coulomb - Eikonal Approximation* ; Sep. 1991

NIFS-107 S. Murakami and T. Sato, *Macroscale Particle Simulation of Externally Driven Magnetic Reconnection;* Sep. 1991

NIFS-108 Y. Ogawa, T. Amano, N. Nakajima, Y. Ohyabu, K. Yamazaki, S. P. Hirshman, W. I. van Rij and K. C. Shaing, *Neoclassical Transport Analysis in the Banana Regime on Large Helical Device (LHD) with the DKES Code;* Sep. 1991

NIFS-109 Y. Kondoh, *Thought Analysis on Relaxation and General Principle to Find Relaxed State;* Sep. 1991

NIFS-110 H. Yamada, K. Ida, H. Iguchi, K. Hanatani, S. Morita, O. Kaneko, H. C. Howe, S. P. Hirshman, D. K. Lee, H. Arimoto, M. Hosokawa, H. Idei, S. Kubo, K. Matsuoka, K. Nishimura, S. Okamura, Y. Takeiri, Y. Takita and C. Takahashi, *Shafranov Shift in Low-Aspect-Ratio Heliotron / Torsatron CHS* ; Sep 1991

NIFS-111 R. Horiuchi, M. Uchida and T. Sato, *Simulation Study of Stepwise Relaxation in a Spheromak Plasma ;* Oct. 1991

NIFS-112 M. Sasao, Y. Okabe, A. Fujisawa, H. Iguchi, J. Fujita, H. Yamaoka and M. Wada, *Development of Negative Heavy Ion Sources for Plasma Potential Measurement* ; Oct. 1991

NIFS-113 S. Kawata and H. Nakashima, *Tritium Content of a DT Pellet in Inertial Confinement Fusion* ; Oct. 1991

NIFS-114 M. Okamoto, N. Nakajima and H. Sugama, *Plasma Parameter Estimations for the Large Helical Device Based on the Gyro-Reduced Bohm Scaling* ; Oct. 1991

NIFS-115 Y. Okabe, *Study of* Au^- *Production in a Plasma-Sputter Type Negative Ion Source* ; Oct. 1991

NIFS-116 M. Sakamoto, K. N. Sato, Y. Ogawa, K. Kawahata, S. Hirokura, S. Okajima, K. Adati, Y. Hamada, S. Hidekuma, K. Ida, Y. Kawasumi, M. Kojima, K. Masai, S. Morita, H. Takahashi, Y. Taniguchi, K. Toi and T. Tsuzuki, *Fast Cooling Phenomena with Ice Pellet Injection in the JIPP T-IIU Tokamak;* Oct. 1991